Transfer of Rolf S3-S4 Linker to hERG Eliminates Activation Gating but Spares Inactivation

Frank S. Choveau,[†‡§] Aziza El Harchi,[†‡§] Nicolas Rodriguez,[†‡§] Bénédicte Louérat-Oriou,[†‡§] Isabelle Baró,[†‡§] Sophie Demolombe,[†‡§] Flavien Charpentier,[†‡§¶] and Gildas Loussouarn[†‡§*]

[†]INSERM, UMR915, Nantes, F-44035, France; [‡]CNRS, ERL3147, Nantes F-44035, France; [§]Université de Nantes, Faculté de Médecine, l'institut du thorax, Nantes, F-44035, France; and [¶]CHU Nantes, l'institut du thorax, Nantes, F-44000, France

ABSTRACT Studies in *Shaker*, a voltage-dependent potassium channel, suggest a coupling between activation and inactivation. This coupling is controversial in hERG, a fast-inactivating voltage-dependent potassium channel. To address this question, we transferred to hERG the S3-S4 linker of the voltage-independent channel, rolf, to selectively disrupt the activation process. This chimera shows an intact voltage-dependent inactivation process consistent with a weak coupling, if any, between both processes. Kinetic models suggest that the chimera presents only an open and an inactivated states, with identical transition rates as in hERG. The lower sensitivity of the chimera to BeKm-1, a hERG preferential closed-state inhibitor, also suggests that the chimera presents mainly open and inactivated conformations. This chimera allows determining the mechanism of action of hERG blockers, as exemplified by the test on ketoconazole.

INTRODUCTION

The human ether-à-go-go-related gene *KCNH2* encodes the α-subunit of the ion channel (hERG) underlying the cardiac delayed rectifier K^+ current, I_{Kr} (1). hERG is a member of the voltage-gated K^+ (Kv) channel family. Similar to other Kv, its α-subunit contains six putative transmembrane segments (S1-S6), a P-loop, several charged residues in segments S2 and S3, and positively charged residues in S4 that are conserved among voltage-gated channels (2). The presence of a cyclic nucleotide binding site in its C-terminal end suggests that it derives from a common evolutionary ancestor with the superfamily of cyclic nucleotide-gated channels (3). In the human heart, I_{Kr} plays a prominent role in the phase 3 of the action potential and not during the phase 1 or 2 when fast inactivation limits the contribution of I_{Kr} to repolarization. This profile is due to the unusual kinetics of hERG gating, with slow activation and fast inactivation (1). Despite its unusual kinetic properties and intrinsic voltage dependence, hERG inactivation is termed C-type because of its sensitivity to TEA^+ (4).

Hoshi et al. (5) studied the properties of the C-type inactivation process in *Shaker*, another voltage-dependent K^+ channel. They have shown that the time constant of C-type inactivation is voltage independent between −25 and +50 mV. They concluded that if this voltage independence is maintained at lower voltages, C-type inactivation is not intrinsically voltage-dependent and must be partially coupled to activation. More recently, Panyi and Deutsch (6) have shown in *Shaker* that the rate of activation depends on the state of the inactivation gate, suggesting that activation and inactivation are coupled. For hERG, the coupling of activation and inactivation processes remains controversial (7,8). One way to address this question would be to use a mutant of hERG stabilized in the activated configuration and to study the impact on the inactivation process. The mutation D540K in the S4-S5 linker of the hERG channel causes a stabilization in the open state at negative voltages (9). The drastic changes in its activation properties are accompanied with a moderate change in its inactivation properties, suggesting a weak coupling between activation and inactivation processes. The D540K mutation may not, however, be the most relevant to test this coupling because the S4-S5 linker interacts with the pore domain (10). Because hERG inactivation results from a modification of the pore conformation, the observed effect of the mutation on inactivation may be direct, and not through activation. Consistent with this, the D540K channel shows a decreased sensitivity to MK-499, a blocker of hERG, known to interact with the pore lining S6 domain (11). Thus, stabilizing hERG in the open configuration without directly modifying the pore structure may require modifying a region further from the pore. In an attempt to prevent a direct effect on inactivation and to specifically target the S4 functionality, by supposedly constraining its movement, we mutated the S3-S4 region that is far from the pore domain, based on the Kv1.2 structure (12).

In 1997, a study by Tang and Papazian (13) showed that the voltage independence of the cyclic nucleotide-gated channel rolf (''rat olfactory channel'') can be transferred to *Drosophila* eag, the ether-à-go-go channel, by replacing the eag S3-S4 loop by the corresponding rolf S3-S4 loop. When transferred into eag, the S3-S4 loop of rolf increases the stability of the open conformation and shifts the voltage

Submitted June 3, 2008, and accepted for publication May 28, 2009.

Frank S. Choveau and Aziza El Harchi contributed equally to the work.

*Correspondence: gildas.loussouarn@nantes.inserm.fr

Aziza El Harchi's present address is Department of Physiology and Pharmacology, School of Medical Sciences, University of Bristol, Bristol BS8 1TD, UK.

Editor: Toshinori Hoshi.

0006-3495/09/09/1323/12 $2.00

doi: 10.1016/j.bpj.2009.05.060

dependence of activation to very hyperpolarized potentials. We hypothesized that replacing the hERG S3-S4 loop by the rolf S3-S4 loop would stabilize the channel in the same manner as in the eag chimera channel. We made such a chimera and the channel obtained barely deactivates, consistent with the hypothesis. The modification of the activation process does not modify the voltage dependence and the kinetics of inactivation. These results suggest a weak coupling, if any, between activation and inactivation in hERG channels. In the physiological range of the cardiac action potential (from −90 to + 30 mV), the chimeric channel seems to present only two conformations: open and inactivated.

This chimera may be useful to accurately characterize the state-dependent block of hERG inhibitors and discriminate possible affinity for the closed state. The mechanism of hERG inhibition by ketoconazole remains controversial (14–16). We took the opportunity of this chimeric channel to study the inhibition by ketoconazole. This drug has been described successively as a preferential closed-state blocker (14,16) and as a preferential open or inactivated-state blocker (15). The use of the chimera shows that ketoconazole preferentially inhibits open and inactivated hERG channels.

METHODS

Molecular biology

The chimera was constructed by three-step PCR. The DNA sequence encoding the hERG S3-S4 linker (NH2-SGSEELIGLL-COOH) was replaced by that of rolf (rat olfactory potassium channel) (NH2-AVGIHSPEV-COOH) using the following primers (5′-GCAGTAGGAATTCATTCACCAGAAGTAAAGA CTGCGCGGCTGCTGCGGCT GGTGCGC-3′; 5′-GGGAGATCTTCTCT GAGTTGGTGTTGG-3′). The PCR product was purified by agarose gel electrophoresis (DNA extraction kit; Qiagen, Courtaboeuf, France), sequenced and then cloned into pIRES-CD8.

Cell culture and transfection

African green monkey kidney fibroblast-like cell line (COS-7) was obtained from the American Type Culture Collection (Rockville, MD) and cultured as described previously (17). Cells were transfected with DNA (2 μg/mL of culture medium) complexed to JetPEI (Polyplus-Tranfection, Strasbourg, France) according to the manufacturer's instructions. Eight hours later, the cells were isolated, diluted, and seeded in 35-mm petri dishes. In hERG experiments, COS-7 cells were cotransfected with 0.8 μg of hERG (pSI hERG) (18) and 1.2 μg of pEGFP (Clontech, Palo Alto, CA) coding for the green fluorescence protein. In chimera experiments, COS-7 cells were transfected with 2 μg of pIRES-chimera-CD8. Dynabeads CD8 (Invitrogen Dynal AS, Norway) were used to identify the cells expressing the chimera. hERG and the chimeric channel densities at the sarcolemma were probably equivalent because the current densities were not significantly different (unpaired *t*-test; hERG: 22 ± 7 pA/pF, $n = 8$; chimera: 19 ± 6 pA/pF, $n = 8$).

Patch-clamp recordings

Ion currents from hERG- and chimera-transfected COS-7 cells were recorded using the whole-cell configuration of the patch-clamp technique. Cells were placed on the stage of an inverted microscope and continuously superfused with the standard extracellular medium. Patch pipettes with a tip resistance of 2.5–5 MΩ were electrically connected to a patch-clamp amplifier (Axopatch 200A; Axon Instruments, Foster City, CA). Stimulation, data recording, and analysis were carried out through an A/D converter (Tecmar TM100 Labmaster; Scientific Solutions, Solon, OH) and using Acquis1 software (Bio-Logic, Claix, France). A microperfusion system allowed local application and rapid change of the different experimental solutions. The cell capacitance was determined by analyzing the capacitive current recorded during a step to −70 mV applied for 50 ms from a holding potential of −60 mV. Current values were normalized using cell capacitance. For inactivation and recovery from inactivation studies, capacitance and series resistance were electronically compensated.

To study the voltage dependence of hERG and the chimera activation, membrane potential was stepped, in 10-mV decrements, from a holding potential of −80 mV to various voltages between +50 mV and −130 mV, and then back to −60 mV, every 3500 ms (Fig. 1).

The voltage dependence of hERG activation was determined by fitting the normalized tail current (*Itail*) versus prepulse voltage (*Vpp*) relationship with a Boltzmann equation:

$$Itail/Itail\,\max = 1/(1 + \exp(-(Vpp - V_{0.5})/k)), \quad (1)$$

where *Itail* max is the maximum tail current, $V_{0.5}$ is the half-activation potential, and k, the slope factor. The time constants of deactivation ($\tau 1$ and $\tau 2$) were determined by a two-exponential fit to the tail current using the following equation:

$$I/I_p = A1 \times \exp(-t/\tau 1) + A2 \times \exp(-t/\tau 2) + I_{ss}, \quad (2)$$

where I represents the current amplitude at time t, I_p is the peak tail current, $\tau 1$ and $\tau 2$ are the time constants for the fast and slow components of the deactivating current, A_1 and A_2 are the relative amplitude of each component, and I_{ss} the relative residual current component.

hERG inactivation was studied with two different three-pulse protocols (Fig. 2). In the first protocol (Fig. 2 *A*), hERG-expressing cells were repolarized (second pulse) for 5 ms to allow recovery from inactivation, with minimum deactivation. Voltage dependence of hERG or chimera inactivation was observed during the third voltage pulse. This protocol allowed measuring the inactivation rate constant at various membrane potentials, and to establish the inactivation curve, but only at potentials at which deactivation is slow (>−60 mV). The second protocol (see Fig. 2 *C* and Zou et al. (8)) enables compensation for the fraction of deactivation at potentials lower than −60 mV during the second step. During this step, recovery from inactivation is faster and distinguishable from deactivation. Deactivation is thus evaluated from the decreasing part of the current during this step, and compensated. The voltage dependence of inactivation was determined by fitting the relative inactivating currents at +60 mV versus voltage with a Boltzmann equation similar to Eq. 1.

Recovery from inactivation was evaluated using a two-pulse protocol (Fig. 3).

The time constants of inactivation (τ_{inact}) and recovery from inactivation ($\tau_{rec\ inact}$) were measured using a single-exponential fit to the tail current using the following equation:

$$I = A \times \exp(-t/\tau) + C, \quad (3)$$

where I represents current amplitude at time t, τ is the time constant of inactivation or recovery from inactivation, $C + A$ represents the initial current amplitude, and C describes the current amplitude after inactivation/recovery from inactivation. Kinetics of recovery from inactivation were fitted on the first 2–10 ms.

All experiments were carried out at 35°C. Patch-clamp data are presented as mean ± SE. Statistical significance of the observed effects was assessed by means of unpaired or paired Student's *t*-tests, one-way, or two-way analysis of variance with a Tukey test when needed. A value of $p < 0.05$ was considered significant.

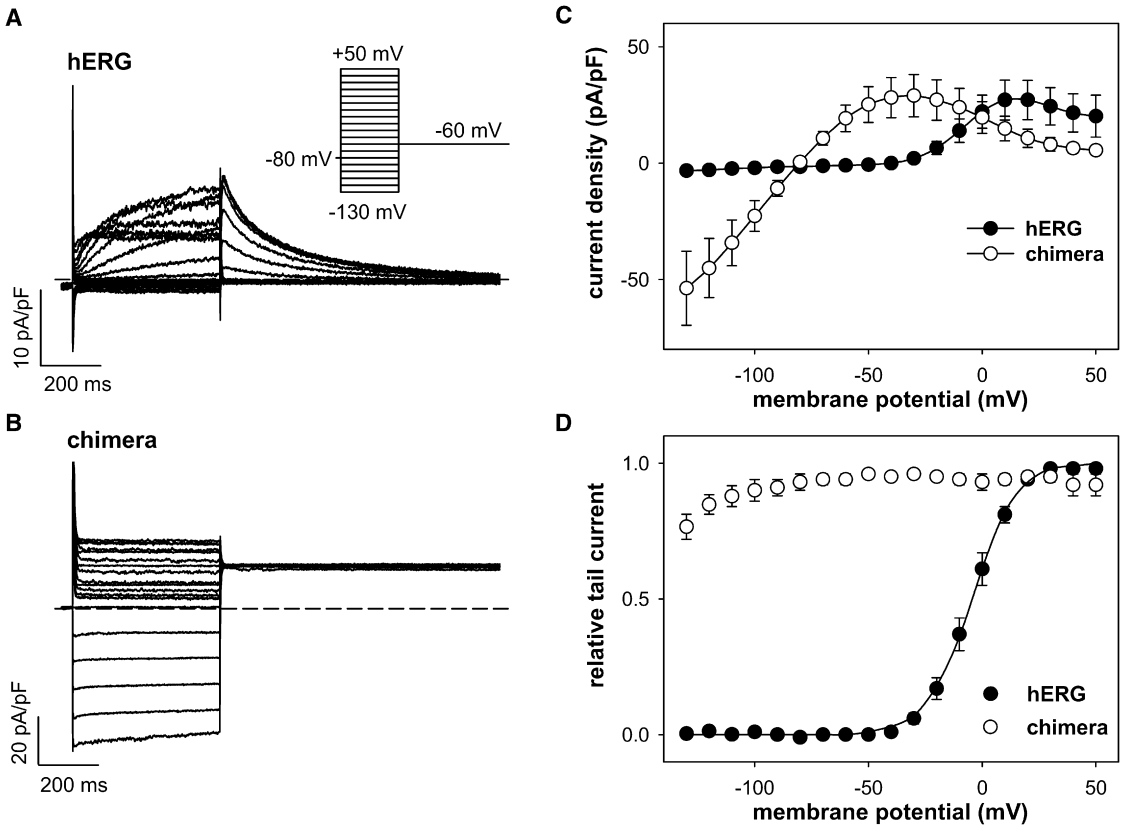

FIGURE 1 Voltage dependence of hERG and the chimera activation. Representative whole-cell current recordings from COS-7 cells expressing (*A*) wild-type hERG or (*B*) chimeric channels. (*Inset*) Voltage stimulation, every 3.5 s. (*C*) Current density measured at the end of the prepulse versus voltage in cells expressing hERG ($n = 8$) or chimeric ($n = 8$) channels. (*D*) Relative tail current measured at −60 mV versus prepulse potential in cells expressing hERG ($n = 8$) or chimeric ($n = 8$) channels. hERG steady-state activation was determined by fitting hERG data with a Boltzmann function (*solid line*).

E-4031 dose-response curves were fitted using the modified Hill equation:

$$y = 1 - d + d/\left(1 + (x/\mathrm{IC}_{50})^{h}\right), \quad (4)$$

where d is the fraction of current that is sensitive to E-4031, x is the drug concentration, h the Hill coefficient, IC_{50} is the concentration at which the half-maximal peak tail currents were obtained, and y is the fraction of current remaining at concentration x of E-4031.

Solutions and drugs

The standard extracellular medium contained 145 mM NaCl, 4 mM KCl, 1 mM $MgCl_2$, 1 mM $CaCl_2$, 5 mM HEPES, and 5 mM glucose, pH adjusted to 7.4 with NaOH. The intracellular medium contained 74.5 mM KCl, 70.5 mM K-aspartate, 5 mM HEPES, 2 mM EGTA, 2 mM K_2ATP, and 0.3 mM $MgCl_2$ pH 7.2 with KOH. All products are from Sigma-Aldrich (St. Quentin Fallavier, France).

Ketoconazole (Sigma-Aldrich Chimie) was dissolved in DMSO to produce a 10-mM stock solution stored at −20°C and further diluted in extracellular medium. Recombinant BeKm-1 toxin (rBeKm-1, Alomone, Israel) was dissolved in 10 mM Tris-HCl, 1 mM EDTA, pH 7.6 to produce a 25 μM stock solution stored at −20°C. Final experimental concentration was reached by dilution in the locally perfused extracellular medium: 145 mM NaCl, 4 mM KCl, 1 mM $MgCl_2$, 1 mM $CaCl_2$, 5 mM HEPES, 5 mM glucose, and 30 mM mannitol, pH adjusted to 7.4 with NaOH. In 100 mM $[K+]_o$ solution, 96 mM NaCl was replaced by KCl.

E-4031 (Sigma-Aldrich Chimie) was dissolved in water to produce a 10-mM stock solution stored at −20°C and further diluted in the locally perfused extracellular medium for final experimental concentration.

Kinetic models

The Markov state model for hERG (Fig. 4 *B*) was adapted from Clancy and Rudy (19). The single open state was named *O*, the inactivated state *I*, and closed states *C1–C3*. Currents were computed according to $I = N \times g \times P_O \times (Vm - Vi)$, where I is the current, $N \times g$ represents the maximal conductance of the membrane, and P_O, the open probability. The parameter $N \times g$ and the transition constants were optimized to simulate a representative recording. The inversion potential Vi was set to −80 mV. Optimization was carried out with ModelMaker v4.0 (AP Benson, Wallingford, UK) using the Marquardt method.

RESULTS

The rolf-hERG S3-S4 chimera is activated at negative potentials

On transfection with hERG cDNA, COS-7 cells expressed a large K^+ current with biophysical properties reminiscent of the rapid component of the human cardiac delayed rectifier K^+ current (Fig. 1 *A*) (20). A slowly activating K^+ current developed during depolarizations above −40 mV with a maximum at a potential between +10 and +20 mV in hERG-expressing cells (Fig. 1, *A* and *C*). With further depolarization, the current amplitude decreased progressively. This inward rectification of hERG is due to the

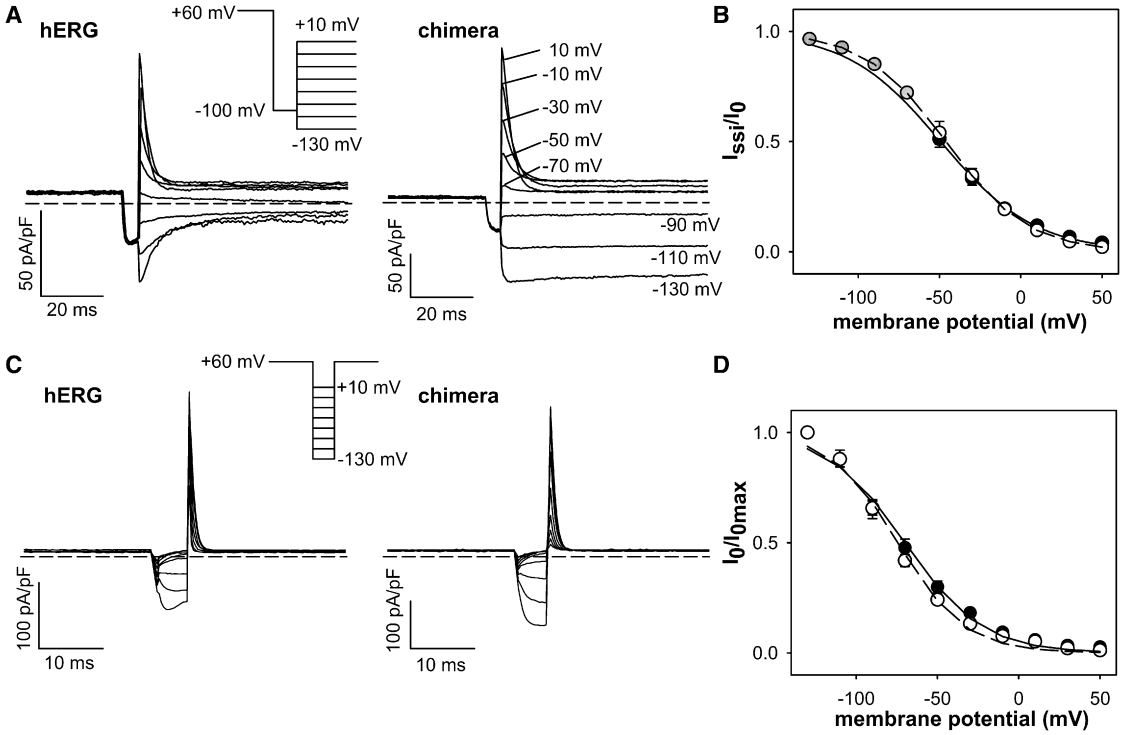

FIGURE 2 hERG and the chimera have identical inactivation. (*A* and *C*) Representative inactivating current recordings of cells expressing hERG or chimeric channels recorded with two protocols. (*Inset*) Three-pulse voltage protocol from holding potential −80 mV. Pulses duration: (*A*) first, 200 ms; second, 5 ms; third, 200 ms, every 3 s; (*C*) first, 1000 ms; second, 5 ms; third, 50 ms, every 3 s. (*B*) Steady-state current (I_{ssi} measured 20 ms after the beginning of the pulse) relative to the peak current (I_0) recorded during the third pulse versus voltage in cells expressing hERG ($n = 8$) or chimeric ($n = 7$) channels. Steady-state inactivation was determined by fitting the data (WT, *solid circle*; chimera, *open circle*; measured values that are not taken into account for the fit, *gray circles*) with a Boltzmann function (*solid line*). (*D*) Peak current (I_0) relative to maximal peak current (I_{0max}) estimated by fitting current traces 1 ms after depolarization and extrapolating to the beginning of the pulse (hERG, $n = 6$; chimera, $n = 7$). In the case of hERG current, I_0 is corrected from the fraction of deactivation measured during the second pulse. Steady-state inactivation was determined by fitting the data as in *B*.

channel voltage-dependent inactivation (4,21). Analysis of the tail current allowed us to characterize the half-maximum activation voltage ($V_{0.5}$) and slope factor (k), giving -4.9 ± 2.3 mV and 8.9 ± 0.6 mV ($n = 8$), respectively (Fig. 1 *D*). The hERG deactivation time course was obtained by fitting the decay of tail current at −60 mV after full activation at +20 mV, by a two-exponential function. Time constants were $\tau 1 = 86 \pm 8$ ms and $\tau 2 = 490 \pm 60$ ms and the relative amplitudes of the two components were $A_1 = 0.56 \pm 0.06$ and $A_2 = 0.41 \pm 0.05$, respectively. The relative residual current component was $I_{ss} = 0.03 \pm 0.01$ ($n = 8$).

The same study was undertaken on COS-7 cells expressing the chimera. Unlike hERG channels, chimeric channels produced an instantaneous K^+ current that was observed during hyperpolarized potentials as well as depolarized potentials (Fig. 1, *B* and *C*). The tail current displayed no deactivation (Fig. 1 *B*) and the activation curve was voltage independent (Fig. 1 *D*). These results show clearly that the chimera deactivation process is impaired, as it is in the case of the rolf-eag chimera (13). However, an inward rectification was still detected at more positive potentials with a maximum current recorded at more negative potentials (~−30 mV) than for hERG current (between +10 and +20 mV) (Fig. 1 *C*).

Voltage-dependent inactivation is conserved in the rolf-hERG S3-S4 chimera

Alteration of the activation process would not necessarily be expected to affect inactivation. This is suggested by the preservation of an inward rectification in the chimera. To accurately check for a potential modification of the inactivation process, the voltage dependence of hERG and chimeric channel inactivation were compared. Because it is difficult to measure steady-state inactivation on hERG, because of concomitant deactivation, two three-pulse protocols were used (Fig. 2) (8,21,22). In the first protocol (Fig. 2 *A*), hERG currents were activated by a 200-ms depolarizing step to +60 mV. The cell was then repolarized to −100 mV for 5 ms to allow recovery from inactivation. Finally, a test step was applied to different voltages to observe the current inactivation kinetics. Fig. 2 shows hERG and the chimera voltage dependence of inactivation. hERG currents recorded during the test step were of large amplitude and rapidly inactivated. For depolarizations, similar inactivating currents were observed in COS-7 cells expressing the chimera (Fig. 2 *A*). For hyperpolarizations, deactivation was detected only in cells expressing hERG. The half-inactivation

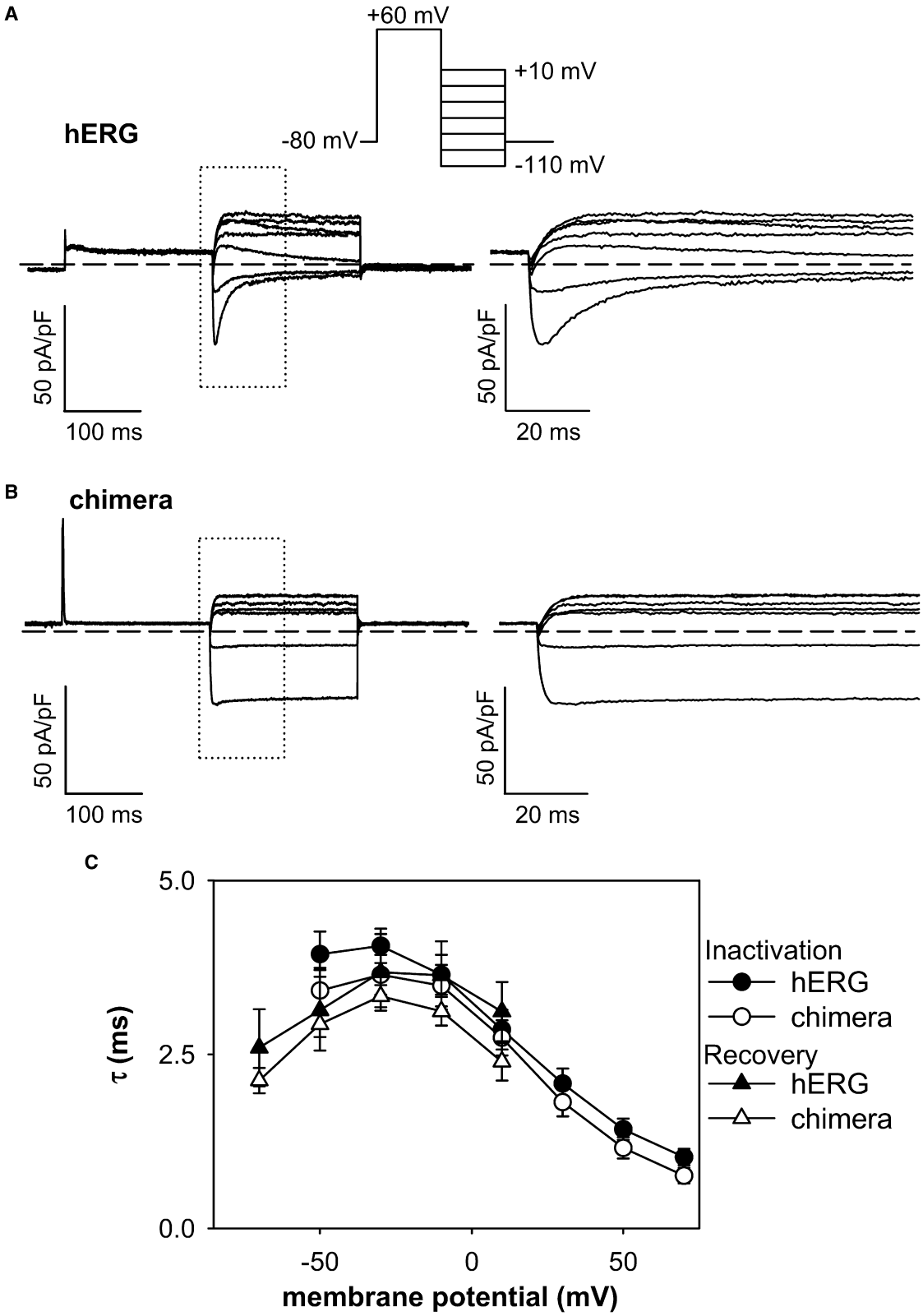

FIGURE 3 hERG and the chimera have identical inactivation and recovery from inactivation kinetics. Recovery from inactivation current traces of (*A*) hERG and the (*B*) chimera. (*Right*) Time-expanded framed zone. (*Inset*) Voltage protocol, every 3 s. (*C*) Voltage dependence of the time constant of recovery from inactivation for hERG ($n = 6$) and the chimera ($n = 7$) and voltage dependence of the inactivation time constant for hERG ($n = 9$) and the chimera ($n = 9$).

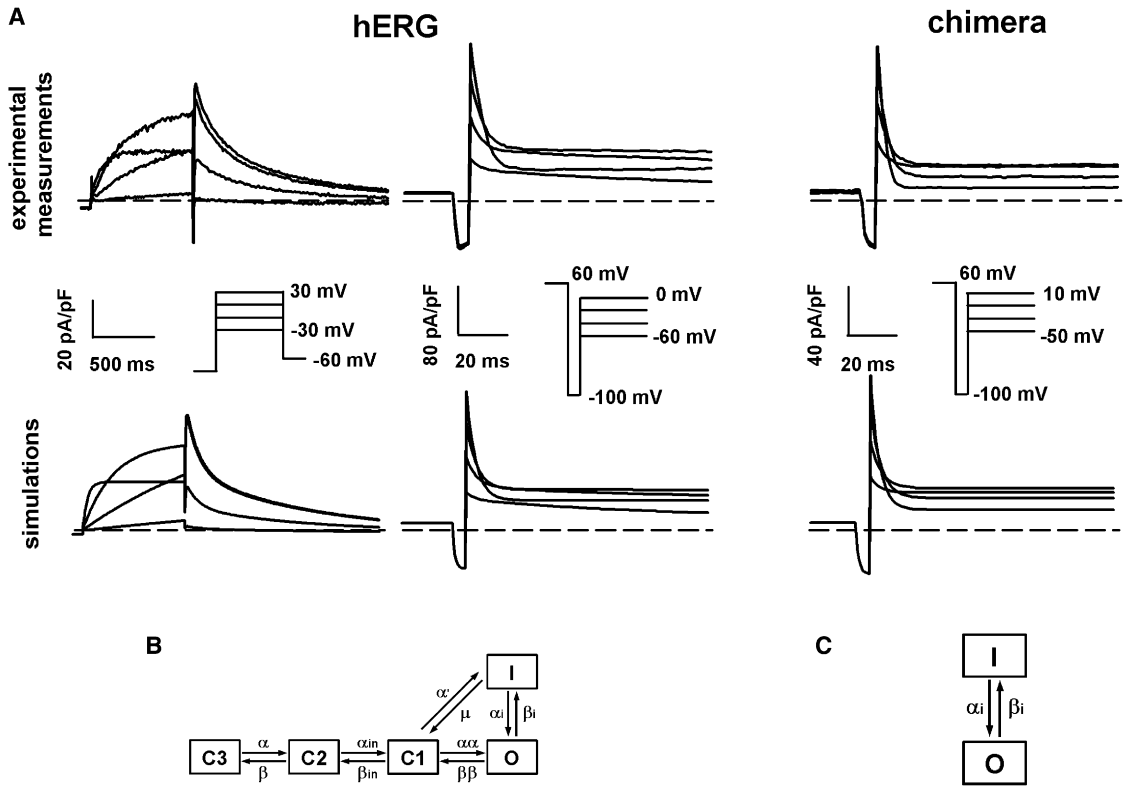

FIGURE 4 Kinetic models of hERG and chimeric channels. (*A*, *top*) Representative whole-cell current recordings from COS-7 cells expressing hERG or chimeric channels. (*Inset*) corresponding voltage protocols. (*A*, *bottom*) Simulated currents obtained with the hERG kinetic model (*B*) optimized to fit hERG experimental currents. (*Right*) Simulated chimera currents were obtained with the chimera kinetic model (*C*) using the same transition rates as the hERG kinetic model. No further optimization was used or needed.

potential ($V_{0.5}$) was evaluated from the remaining current ratio (I_{ssi}/I_0) after 20 ms of inactivation. For hERG, the fit of the inactivation curve was done only with the data measured at potentials >-60 mV. For these potentials, deactivation after 20 ms is small because the fast component time constant of deactivation ($\tau 1$), which represents 56% of the deactivation process, is at least four times >20 ms. For the chimera, the fit was also done only with the data measured at potentials > -60 mV, even though there is no deactivation at lower potentials. However, it can be noticed that the data measured at potentials lower than -60 mV (Fig. 2 *B*, *gray circles*) are well fitted by the Boltzmann curve. $V_{0.5}$ were -50 ± 4 mV ($n = 8$) and -47 ± 5 mV ($n = 7$; unpaired *t*-test: not significant (NS)) for hERG and the chimera, respectively. The corresponding k values were $k = 29 \pm 1$ mV ($n = 8$) and $k = 25 \pm 2$ mV ($n = 7$; unpaired *t*-test: NS) for hERG and the chimera, respectively. To circumvent the bias on inactivation measurement due to fast deactivation at potentials lower than -60 mV, we used another three-pulse protocol (Fig. 2, *C* and *D*). The second step at various potentials (+70 to -130 mV) allows the recovery from inactivation and the measurement of the fraction of deactivation (see Methods). The initial current of the third step at +60 mV is proportional to the degree of inactivation at the end of the second step (after correction of deactivation). The half-inactivation potential ($V_{0.5}$) was evaluated from the fit of the inactivating current recorded during the third step. $V_{0.5}$ were -71 ± 4 mV ($n = 6$) and -74 ± 2 mV ($n = 7$; unpaired *t*-test: NS) for hERG and the chimera, respectively. The corresponding k values were $k = 23 \pm 1$ mV ($n = 6$) and $k = 21 \pm 1$ mV ($n = 7$; unpaired *t*-test: NS) for hERG and the chimera currents respectively. The two protocols used did not give similar $V_{0.5}$ values. One reason is that the second protocol does not allow measurements of steady-state inactivation at several potentials: at -10 to -50 mV, recovery from inactivation is slightly too slow (Fig. 3 *C*) to reach a steady-state during the 5-ms pulse. Nevertheless, our results show that the voltage dependences of hERG and the chimera currents are similar, whatever protocol was used.

The first three-pulse protocol allowed us to compare the time constant of inactivation for hERG and the chimera. The averaged data are plotted in Fig. 3 *C*. The superimposition of the results shows that the voltage dependence of inactivation kinetics is not modified in the chimera.

For hERG, the prepulse used for recovery from inactivation can not exceed 5 ms at -100 mV to have minimal deactivation whereas almost complete recovery from inactivation. The absence of deactivation in the chimera allowed us to test whether a longer prepulse (30 ms) impacts inactivation. The value of $V_{0.5}$ as well as the inactivation kinetics values were

not modified and were identical to hERG values (see Fig. S1 in the Supporting Material). It can also be noticed that a weak deactivation could be detected for the chimera current at very negative potentials only (−130 mV; Fig. 2 *A* and Fig. S1) indicating a large shift of the activation curve toward very negative potentials. The decrease in the tail current cannot be a consequence of extracellular K^+ depletion due to large K^+ influxes during the very negative prepulses (between −130 mV and −110 mV). Such extracellular K^+ depletion would cause a shift of E_K to a potential more negative than −80 mV, leading to an increase (and not a decrease) of the tail current measured at −60 mV (Fig. 1 *D*).

Recovery from inactivation was studied using a two-pulse protocol (Fig. 3) as in other works (21,23). This protocol generated the rapid recovery of hERG current followed by deactivation. As for inactivation, chimera and hERG recoveries from inactivation were similar (Fig. 3 *C*). Again, a slight deactivation of the chimera current could be detected at −130 mV only.

Several studies have shown that a high $[K^+]_o$ strongly slowed the inactivation kinetics in hERG channel (24,25). If the inactivation process is not modified in the chimera, increasing $[K^+]_o$ should lead to the same effect as in WT hERG. To check this hypothesis, we compared the effect of 100 mM $[K^+]_o$ on the chimera and hERG inactivation. We observed that increasing $[K^+]_o$ from 4 to 100 mM strongly slowed the inactivation kinetics of hERG, as previously showed (n = 8–9, two-way ANOVA, with a Tukey test, $p < 0.05$). We observed similar effects on the chimera (n = 8–9, two-way ANOVA, with a Tukey test, $p < 0.05$). There was no significant difference between the effects of $[K^+]_o$ on hERG and the chimera ($n = 8$, two-way ANOVA, NS).

Several studies showed that a high $[K^+]_o$ caused a shift of the voltage-dependence of inactivation toward positive potentials (8,24). We did not observe such a modification, probably because of difference in the temperature and cellular models used. The absence of effect was also observed in the chimera (Fig. S2). Altogether, the results with 100 mM $[K^+]_o$ reinforce the idea that the chimera has an intact inactivation process.

A kinetic model also supports an intact inactivation process in the chimera

A more comprehensive way to compare hERG and the chimeric channel inactivation are kinetic models. These models allowed discriminating the effect of the S3-S4 linker substitution on the inactivation and activation processes. First, we optimized a kinetic model (Fig. 4) of the hERG channel bearing three closed states, one open state, and one inactivated state (19,22,26). A comparison between measured and simulated currents (Fig. 4 *A*) and biophysical parameters (Fig. S3) shows that this model accounts very well for our experimental data. Transition rate values are listed in Table 1. Noticing that the chimera currents can be roughly modeled with a two-state model, we checked whether the transition between these two states might correspond to the *O-I* transition of the hERG channel. Simulated currents for the chimera were obtained with the chimera model (Fig. 4 *C*) using the values of the transition rates (αi and βi) derived from hERG model optimization. Measured chimera currents and biophysical parameters were rather well fitted by this prediction in the range of physiological voltages, without further optimization (Fig. 4 *A* and Fig. S3). This result reinforces the proposition of an intact inactivation transition in the chimera, identical to that of the hERG channel. To get an accurate determination of the transition rates, we imposed as many constraints as possible by fitting both the current recordings and the biophysical parameters. However, it is inherent to a 15 free parameters optimization that its solution is not unambiguous and cannot be distinguished easily from others that also give good fits of the data. In the framework of the model of hERG transitions that we used, it is noteworthy that the *O-I* transition rates strongly determine the inactivation kinetics. The very good fits of the inactivation and recovery from inactivation time constants (Fig. S3) suggest that the determination of *O-I* transition rates for hERG is reasonably accurate. The conclusion regarding the conservation of the *O-I* transition rates between hERG and the chimera should thus be robust despite uncertainties coming from the optimization process.

TABLE 1 hERG and the chimera transition rates (ms^{-1})

hERG transition rates (ms^{-1})	
α	$2.987 \times 10^{-3} \exp(9.377 \times 10^{-2} \times V_m)$
β	1.872×10^{-2}
αin	5.755×10^{-1}
βin	1.056×10^{-1}
$\alpha\alpha$	$1.55 \times 10^{-2} \exp(2.464 \times 10^{-2} \times V_m)$
$\beta\beta$	$1.7 \times 10^{-3} \exp(-2.37 \times 10^{-2} \times V_m)$
α'	$1.579 \times 10^{-1} \exp(6.509 \times 10^{-2} \times V_m)$
μ	$=(\alpha' \times \alpha i \times \beta\beta)/(\alpha\alpha \times \beta i)$
hERG and the chimera transition rates (ms^{-1})	
αi	$4.0 \times 10^{-2} \exp(-3.0 \times 10^{-2} \times V_m)$
βi	$2.3 \times 10^{-1} \exp(1.6 \times 10^{-2} \times V_m)$

V_m, membrane potential (mV).

Chimera inhibition by BeKm-1 is voltage-independent

The chimera kinetic model suggests that the chimera exists in two conformations: open and inactivated. To test this hypothesis, we studied BeKm-1 effects on the chimera and hERG (Fig. 5). BeKm-1 binds to the external face of the hERG channel and has been shown to exhibit preferential closed-state blockade (27,28). A 12-s ascending voltage ramp was applied in baseline conditions. In these conditions, hERG current developed from −40 mV with maximum amplitude at ~0 mV. With further depolarization, the current amplitude decreased progressively (Fig. 5 *A*). The chimera was already activated at the beginning of the ramp (−80 mV), generating a maximum current at ~−40 mV, which declined due to

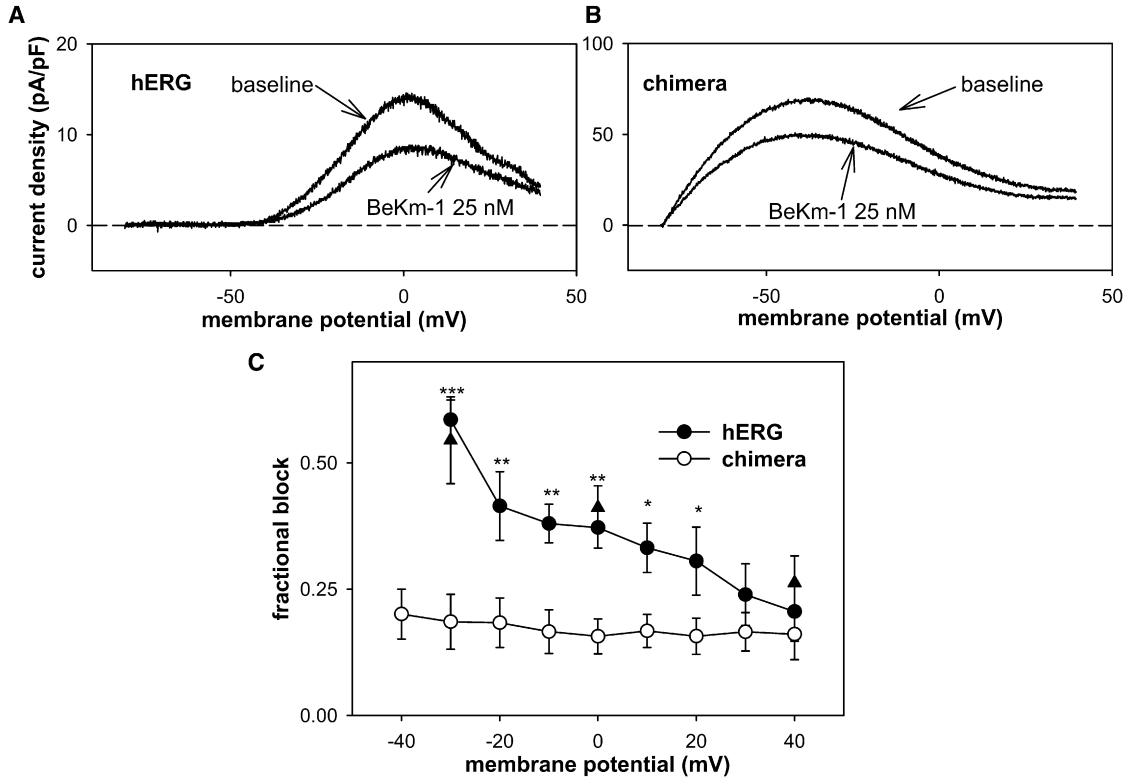

FIGURE 5 Effect of BeKm-1 on hERG and the chimera. Representative currents of (*A*) hERG and the (*B*) chimera in baseline conditions and after a 3-min exposure to 25 nM BeKm-1 elicited by an ascending voltage ramp (10 mV/s; every 15 s). (*C*) Mean fractional block (1 − (current in the presence of 25 nM BeKm-1/baseline current)) measured at various potentials during the depolarizing ramp in cells expressing hERG ($n = 6$) or chimeric ($n = 7$) channels. *$p < 0.05$; **$p < 0.01$; ***$p < 0.001$. (*Solid triangles*) Mean steady-state fractional block measured at the end of a 5-s step to −30 mV ($n = 6$), 0 mV ($n = 7$), or +40 mV ($n = 7$) in cells expressing hERG.

inactivation (Fig. 5 *B*). Then, ramp stimulation was stopped, membrane potential was clamped at −80 mV, and 25 nM BeKm-1 was applied. After 3 min of exposure to the toxin, the stimulation was applied again and the first recorded current ramp was used to evaluate BeKm-1 effects (15). As summarized in Fig. 5 *C*, inhibition of hERG by BeKm-1 was higher at negative voltages and declined at more positive voltages. ANOVA analysis of BeKm-1 inhibition at the different voltages showed a significant voltage-dependence of the block ($n = 6$, one-way repeated measures ANOVA; $p < 0.001$). To check whether the ramp was slow enough to look at the steady-state block, 5-s steps at −30, 0, or +40 mV were also applied from a holding potential of −80 mV in the same conditions (28). The steady-state fractional block measured with the step protocol was similar (Fig. 5 *C*) showing that the ramp was slow enough to get the steady-state block. As opposed to hERG, the chimera was weakly inhibited by BeKm-1 and this inhibition was voltage-independent (NS). Fractional block of the chimera significantly differed from WT at potentials between −30 mV and +20 mV (two-way ANOVA, with a Tukey test) and were similar at higher potentials, when both channels are inactivated (Fig. 5 *C*). The persistence of a fractional block (~20%) suggests that the toxin can bind not only to closed but also to open and inactivated channels (although with a lower affinity). An alternative hypothesis would be the persistence of a closed state in the chimeric channel, allowing toxin binding. A direct measurement of channel open probability by using single channel methods will be necessary to discriminate one of the two hypotheses.

Sensitivity to E-4031 suggests an intact pore in the chimera

We described a hERG mutant (D540K) that was activated at hyperpolarizing potentials (see Introduction). This mutant may not be relevant to study the coupling between activation and inactivation because the mutation is close to the pore domain, in which conformational changes are associated with both activation and inactivation (9). This is confirmed by the use of methanesulfonanilide blockers such as MK-499 and E-4031. Because these blockers are known to target the hERG pore (29,30), the altered sensitivity to MK-499 confirms the effect of the mutation on the pore domain. We tested the effect of E-4031 to determine if the chimera pore was affected similarly to the D540K mutant. In these experiments, hERG and the chimera currents were elicited by a 500-ms depolarizing pulse to +10 mV from

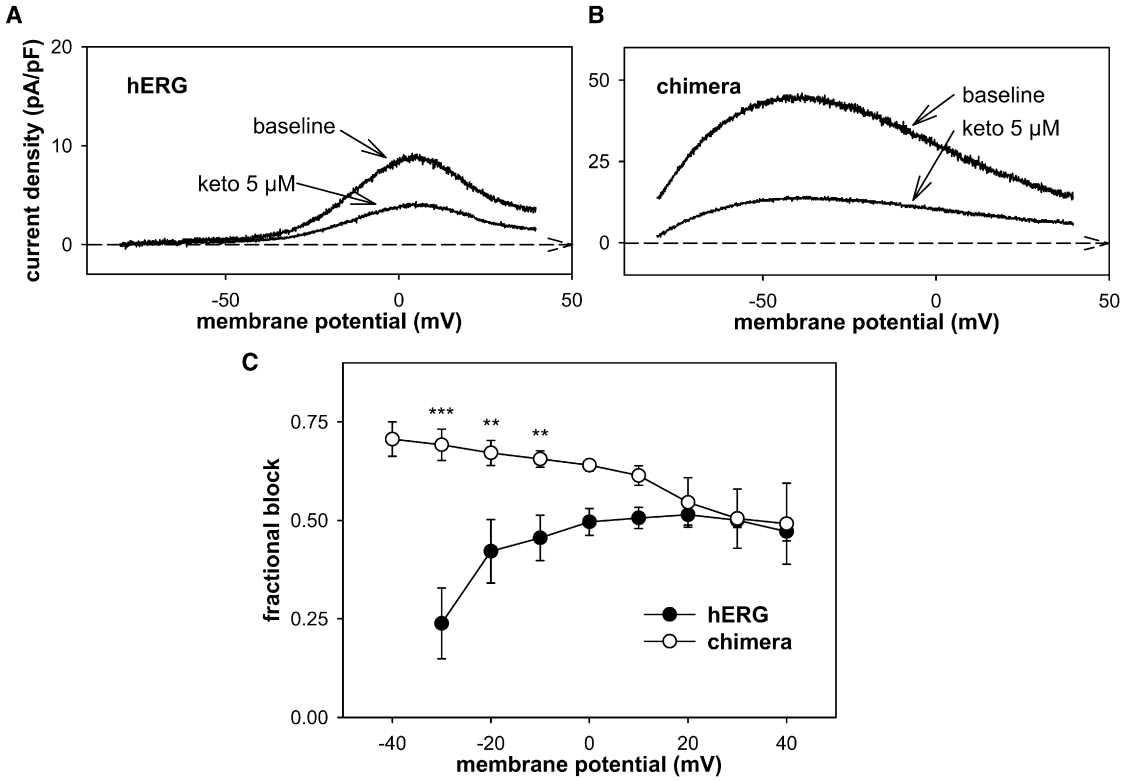

FIGURE 6 Effect of ketoconazole (keto) on hERG and the chimera. Representative currents of (*A*) hERG and (*B*) chimera in baseline conditions and after 3-min exposure to 5 μM keto elicited by an ascending voltage ramp (10 mV/s; every 15 s). (*C*) Mean fractional block (1 − (current in the presence of 5 μM keto/baseline current)) measured at various potentials during the depolarizing ramp in cells expressing hERG ($n = 8$) or chimeric ($n = 6$) channels. $^{**}p < 0.01$; $^{***}p < 0.001$.

a holding potential of −80 mV and the tail current was recorded at −60 mV. Depolarizing steps were applied every 3 s. The dose-response curve for E-4031 inhibition of the tail current showed an IC_{50} of 46 ± 29 nM and a Hill coefficient of 0.72 ± 0.17 for hERG ($n = 6$, data not shown). For the chimera, the IC_{50} was 36 ± 18 nM and the Hill coefficient was 0.89 ± 0.24 ($n = 7$). There was no difference between hERG and the chimera sensitivity to E-4031 (Student's *t*-test, NS). This result confirms that only deactivation is altered in the chimera and that the inactivation and pore are intact.

The chimera indicates that ketoconazole binds preferentially to the open and inactivated states

This preliminary validation of the chimera model to study hERG pharmacology allowed us to evaluate the mechanism of hERG inhibition by ketoconazole. Several studies suggest that ketoconazole inhibits hERG preferentially in the closed state (14,16). However, another study has shown that this drug binds preferentially to the open state (15). To determine the mechanism of action of ketoconazole, we tested its effects on hERG and the chimera. The same protocol as with BeKm-1 was applied. The ramp was slow enough to obtain the steady-state block, because ketoconazole block is much faster than BeKm-1 block (15). If ketoconazole binds preferentially the closed state, we should observe a higher hERG inhibition at negative voltages, which declines at more positive voltages and a weak inhibition of the chimera in the presence of the drug. Contrarily to this hypothesis, but in agreement with Ridley and coworkers, hERG inhibition increased progressively with the potential, reaching a maximum at 0 mV (one-way repeated measures ANOVA; $p < 0.001$) (Fig. 6, *A* and *C*). The difficulty with hERG is that small current amplitude prevents an accurate measurement of the fractional block, particularly at -40 or -30 mV in some cells due to low activation. Because of its full activation, the chimera allowed a more accurate estimation of this fractional block at negative voltages. The chimera was strongly inhibited whatever the voltage was (Fig. 6, *B* and *C*). Fractional block of the chimera significantly differed from hERG at potentials between −30 mV and −10 mV (two-way ANOVA, with a Tukey test). The much lower ketoconazole block of hERG at negative potentials indicates that ketoconazole binds less to hERG closed state than open and inactivated ones.

DISCUSSION

Transfer of voltage independence from rolf to hERG

In this study, we described the biophysical properties of a rolf-hERG S3-S4 chimera. Our results show that only the

activation process is impaired. The voltage dependence of inactivation is conserved because the chimera has the same inactivation and recovery from inactivation properties as the hERG channel. These results show that the modification of the activation process does not modify the inactivation. It seems that activation is not necessary to trigger inactivation. Otherwise, we would observe a change of the inactivation biophysical parameters. To evaluate the effects of the impaired activation on the inactivation process, we optimized the Markov model developed by Clancy and Rudy for hERG kinetics (19). In this model, we convincingly simulated the chimera properties by conserving only the transitions between the open and inactivated states of hERG. We found that the chimera currents are well fitted by this two-state model, reinforcing the hypothesis of a two-state channel. These models are consistent with a weak, if any, relationship between the conformational changes associated with inactivation and those associated with activation because the alteration of the latter in the chimera does not seem to alter the former. However, the models do not exclude that activation and inactivation are indirectly coupled by being both controlled by the movement of the voltage sensor because the hERG model suggests a movement of the voltage sensor (early transitions) followed by movements of the activation and inactivation gates (late transitions). Several studies are consistent with this idea. Loots and Isacoff (31) proposed that, in *Shaker*, activation produces an interaction between S4 and the pore domain. This interaction disrupts the coupling between S5 and S6 domains and leads to inactivation. Regarding hERG, two studies (7,32) suggest that the coupling between the activation and inactivation is mediated by the S4 domain. To probe the voltage-sensor movements, Smith and Yellen (32) used a fluorescence technique to examine the conformational changes of hERG S4. Fluorescent probes attached to three different residues on S3-S4 (E518C, E519C, and L520C) reported both fast and slow voltage-dependent changes in fluorescence. The authors suggested that the fast component corresponds to inactivation, and the slow component to activation. Consequently, it seems that voltage-dependent inactivation is linked to the voltage sensor. However, Hill et al. (33) showed recently that neutralization of the first three charges in the hERG S4 domain (K525Q, R528Q, R531Q) shifts the voltage-dependent activation of 87 mV toward negative potentials but does not modify the voltage-dependent inactivation. These results suggest that unlike activation, hERG inactivation is independent of the S4 movement and reinforce the hypothesis that activation and inactivation are two distinct mechanisms. The same group also carried out an alanine scan of S5 of hERG. Mapping of the functional effect of the mutations on a hERG homology domain clearly shows distinct areas. The residues pointing toward S6 are associated with an altered inactivation process, whereas many residues pointing away and most of the S4-S5 linker are associated with an altered activation process (34). This is also consistent with uncoupled activation and inactivation processes.

Besides an intact inactivation mechanism, the chimera conserves an intact pore as suggested by the comparison of hERG and the chimera blockade by drugs. We tested the sensitivity of the chimera to E-4031 (29) and found that the chimera exhibits the same sensitivity as hERG. The hERG D540K mutant is also activated at hyperpolarized potentials but conserves the ability to activate and inactivate in response to membrane depolarization (9). However, unlike the chimera, this mutant has modified inactivation and a lower sensitivity to MK-499, another methanesulfonanilide (11). The differences between the chimera and the D540K mutant may find their origin in the impairment of distinct mechanisms. In hERG channels, the interaction between the S4-S5 linker (containing D540) and the C-terminal end of the S6 domain allows the coupled movements between the voltage sensor and the activation gate (10). In the D540K mutant, the altered interaction between the voltage sensor and the activation gate may promote channel reopening at hyperpolarized potentials (35). In the chimera, the mechanism involved in the voltage independence of activation may arise from constrained movements of the voltage sensor, upstream of S4-pore coupling. In other words, the S3-S4 substitution would impair the S4 movement but not the coupling between the voltage sensor and the pore. To confirm this hypothesis, gating current measurements will be helpful to determine whether or not the rolf S3-S4 linker limits the movements of the S4 segment in the chimera.

The role of the S3-S4 linker has been studied widely in the *Shaker* channel (36–38). The large deletion of amino acids 333–357 in the S3-S4 linker has only minor effects on the voltage dependence of activation (37). However, amino acids 330–360 deletion leads to a +45-mV shift (36). These results suggest that it is probably not the length of the linker that critically constrains the S4 segment displacement but rather the nature of its amino-acid sequence. We replaced 10 amino acids of hERG S3-S4 linker by nine amino acids of rolf and observed a major effect on activation. Interestingly, this replacement includes amino acid E246 in rolf: substitution of this amino acid to the equivalent position in eag (A345E) has been shown to stabilize the activation gate of the eag (13). To further explore the role of S3-S4 loop in the hERG voltage sensor, a scanning mutagenesis of the S3-S4 loop in the hERG-rolf chimera will allow identifying the specific residues involved in the alteration of the chimera activation.

Use of the chimera as a pharmacological model

Our results show that the chimera has a lower sensitivity to BeKm-1, a blocker that binds preferentially to the channel closed-state. This observation reinforces the idea that the chimera exists mostly in two conformations: open or inactivated. We have used this chimera property to study the

mechanism of ketoconazole action. Two mechanisms have been suggested: a block in the closed state (14,16) or a block in the open or inactivated state (15). We have shown that ketoconazole binds preferentially to the open and inactivated states. This conclusion relies on the assumption that the drug effect on the chimera can be extrapolated to hERG. Two arguments suggest that the binding of ketoconazole to hERG is not modified by the S3-S4 substitution. First, the binding site of ketoconazole does not implicate the S3-S4 linker because it is located in the intracellular part of S6 (15). The second argument is that the effects of ketoconazole on hERG and the chimera are similar at potentials (+20 to +40 mV) at which both channels reside in the same states (open and inactivated).

Focusing on the chimera, fractional block decreased significantly between −40 mV and potentials +20, +30, and +40 mV (one-way repeated measures ANOVA, with a Tukey test), reminiscent of the voltage-dependent block observed with miconazole (39). This may suggest that ketoconazole binds the open channels with a higher affinity than the inactivated channels. However, the voltage dependence of the chimera block does not parallel that of inactivation: the potential for half fractional block is ~0 mV, which is much closer to the half-activation potential (−4.9 mV) than the half-inactivation potential (from −50 to −70 mV depending on the protocol used). This lead to the hypothesis that some structural rearrangements linked to the normal activation process are conserved in the chimera despite the absence of activation gating, and that these rearrangements are responsible for the voltage-dependent interaction of ketoconazole with the chimeric channel.

The mechanism of hERG block by several drugs associated with the acquired long QT syndrome remains unclear. Indeed, moxifloxacin (40), fluvoxamine (41), and, recently, doxepin (42) have been reported to inhibit hERG with a mixed state-dependence of inhibition (with components of both closed- and open-channel block, including a very rapid open-channel block). The results presented in this study suggest that hERG-rolf chimera is a valuable pharmacological model to characterize the state-dependent block and more generally, to identify the mechanism of action of hERG blockers.

SUPPORTING MATERIAL

Three figures are available at http://www.biophysj.org/biophysj/supplemental/S0006-3495(09)01162-X.

We thank Béatrice Leray, Marie-Joseph Louerat, Sylvie Leroux, and Agnes Carcouët for expert technical assistance.

This work was supported by grants from the Institut National de la Santé et de la Recherche Médicale (INSERM) and from the Agence Nationale de la Recherche (ANR-05-JCJC-0160-01 to G.L. and ANR COD/A05045GS to I.B.). F.S.C. is supported by Génavie, the Fondation pour la Recherche Médicale and the Fédération Française de Cardiologie. A.E.H. was the recipient of a grant from INSERM/Pays-de-Loire.

REFERENCES

1. Sanguinetti, M. C., and M. Tristani-Firouzi. 2006. hERG potassium channels and cardiac arrhythmia. *Nature*. 440:463–469.
2. Wei, A., T. Jegla, and L. Salkoff. 1996. Eight potassium channel families revealed by the *C. elegans* genome project. *Neuropharmacology*. 35:805–829.
3. Jan, L. Y., and Y. N. Jan. 1992. Tracing the roots of ion channels. *Cell*. 69:715–718.
4. Smith, P. L., T. Baukrowitz, and G. Yellen. 1996. The inward rectification mechanism of the HERG cardiac potassium channel. *Nature*. 379:833–836.
5. Hoshi, T., W. N. Zagotta, and R. W. Aldrich. 1991. Two types of inactivation in *Shaker* K^+ channels: effects of alterations in the carboxy-terminal region. *Neuron*. 7:547–556.
6. Panyi, G., and C. Deutsch. 2006. Cross talk between activation and slow inactivation gates of *Shaker* potassium channels. *J. Gen. Physiol.* 128:547–559.
7. Piper, D. R., A. Varghese, M. C. Sanguinetti, and M. Tristani-Firouzi. 2003. Gating currents associated with intramembrane charge displacement in HERG potassium channels. *Proc. Natl. Acad. Sci. USA*. 100:10534–10539.
8. Zou, A., Q. P. Xu, and M. C. Sanguinetti. 1998. A mutation in the pore region of HERG K^+ channels expressed in *Xenopus* oocytes reduces rectification by shifting the voltage dependence of inactivation. *J. Physiol.* 509:129–137.
9. Sanguinetti, M. C., and Q. P. Xu. 1999. Mutations of the S4–S5 linker alter activation properties of HERG potassium channels expressed in *Xenopus* oocytes. *J. Physiol.* 514:667–675.
10. Ferrer, T., J. Rupp, D. R. Piper, and M. Tristani-Firouzi. 2006. The S4–S5 linker directly couples voltage sensor movement to the activation gate in the human ether-a′-go-go-related gene (hERG) K^+ channel. *J. Biol. Chem.* 281:12858–12864.
11. Mitcheson, J. S., J. Chen, and M. C. Sanguinetti. 2000. Trapping of a methanesulfonanilide by closure of the HERG potassium channel activation gate. *J. Gen. Physiol.* 115:229–240.
12. Long, S. B., E. B. Campbell, and R. MacKinnon. 2005. Crystal structure of a mammalian voltage-dependent *Shaker* family K^+ channel. *Science*. 309:897–903.
13. Tang, C. Y., and D. M. Papazian. 1997. Transfer of voltage independence from a rat olfactory channel to the *Drosophila* ether-a-go-go K^+ channel. *J. Gen. Physiol.* 109:301–311.
14. Dumaine, R., M. L. Roy, and A. M. Brown. 1998. Blockade of HERG and Kv1.5 by ketoconazole. *J. Pharmacol. Exp. Ther.* 286:727–735.
15. Ridley, J. M., J. T. Milnes, R. S. Duncan, M. J. McPate, A. F. James, et al. 2006. Inhibition of the HERG K^+ channel by the antifungal drug ketoconazole depends on channel gating and involves the S6 residue F656. *FEBS Lett.* 580:1999–2005.
16. Yao, J. A., X. Du, D. Lu, R. L. Baker, E. Daharsh, et al. 2005. Estimation of potency of HERG channel blockers: impact of voltage protocol and temperature. *J. Pharmacol. Toxicol. Methods*. 52:146–153.
17. Loussouarn, G., K. H. Park, C. Bellocq, I. Baro, F. Charpentier, et al. 2003. Phosphatidylinositol-4,5-bisphosphate, PIP2, controls KCNQ1/KCNE1 voltage-gated potassium channels: a functional homology between voltage-gated and inward rectifier K^+ channels. *EMBO J.* 22:5412–5421.
18. Chevalier, P., C. Rodriguez, L. Bontemps, M. Miquel, G. Kirkorian, et al. 2001. Non-invasive testing of acquired long QT syndrome: evidence for multiple arrhythmogenic substrates. *Cardiovasc. Res.* 50:386–398.
19. Clancy, C. E., and Y. Rudy. 2001. Cellular consequences of HERG mutations in the long QT syndrome: precursors to sudden cardiac death. *Cardiovasc. Res.* 50:301–313.
20. Wang, Z., B. Fermini, and S. Nattel. 1994. Rapid and slow components of delayed rectifier current in human atrial myocytes. *Cardiovasc. Res.* 28:1540–1546.

21. Spector, P. S., M. E. Curran, A. Zou, M. T. Keating, and M. C. Sanguinetti. 1996. Fast inactivation causes rectification of the IKr channel. *J. Gen. Physiol.* 107:611–619.

22. Wang, S., M. J. Morales, S. Liu, H. C. Strauss, and R. L. Rasmusson. 1997. Modulation of HERG affinity for E-4031 by [K+]o and C-type inactivation. *FEBS Lett.* 417:43–47.

23. Snyders, D. J., and A. Chaudhary. 1996. High affinity open channel block by dofetilide of HERG expressed in a human cell line. *Mol. Pharmacol.* 49:949–955.

24. Wang, S., S. Liu, M. J. Morales, H. C. Strauss, and R. L. Rasmusson. 1997. A quantitative analysis of the activation and inactivation kinetics of HERG expressed in *Xenopus* oocytes. *J. Physiol.* 502:45–60.

25. Yang, T., D. J. Snyders, and D. M. Roden. 1997. Rapid inactivation determines the rectification and [K+]o dependence of the rapid component of the delayed rectifier K^+ current in cardiac cells. *Circ. Res.* 80:782–789.

26. Kiehn, J., A. E. Lacerda, and A. M. Brown. 1999. Pathways of HERG inactivation. *Am. J. Physiol.* 277:H199–H210.

27. Korolkova, Y. V., G. N. Tseng, and E. V. Grishin. 2004. Unique interaction of scorpion toxins with the hERG channel. *J. Mol. Recognit.* 17:209–217.

28. Milnes, J. T., C. E. Dempsey, J. M. Ridley, O. Crociani, A. Arcangeli, et al. 2003. Preferential closed channel blockade of HERG potassium currents by chemically synthesized BeKm-1 scorpion toxin. *FEBS Lett.* 547:20–26.

29. Sanguinetti, M. C., and N. K. Jurkiewicz. 1990. Two components of cardiac delayed rectifier K+ current. Differential sensitivity to block by class III antiarrhythmic agents. *J. Gen. Physiol.* 96:195–215.

30. Spector, P. S., M. E. Curran, M. T. Keating, and M. C. Sanguinetti. 1996. Class III antiarrhythmic drugs block HERG, a human cardiac delayed rectifier K^+ channel. Open-channel block by methanesulfonanilides. *Circ. Res.* 78:499–503.

31. Loots, E., and E. Y. Isacoff. 2000. Molecular coupling of S4 to a K(+) channel's slow inactivation gate. *J. Gen. Physiol.* 116:623–636.

32. Smith, P. L., and G. Yellen. 2002. Fast and slow voltage sensor movements in HERG potassium channels. *J. Gen. Physiol.* 119:275–293.

33. Hill, A. P., and J. I. Vandenberg. 2008. Investigating the origin of the voltage-sensitivity of inactivation in hERG potassium channels. *Biophys. J.* 94:448–459.

34. Ju, P., G. Pages, R. P. Riek, P. C. Chen, A. M. Torres, et al. 2009. The pore domain outer helix contributes to both activation and inactivation of the HERG K^+ channel. *J. Biol. Chem.* 284:1000–1008.

35. Tristani-Firouzi, M., J. Chen, and M. C. Sanguinetti. 2002. Interactions between S4–S5 linker and S6 transmembrane domain modulate gating of HERG K^+ channels. *J. Biol. Chem.* 277:18994–19000.

36. Gonzalez, C., E. Rosenman, F. Bezanilla, O. Alvarez, and R. Latorre. 2000. Modulation of the *Shaker* K(+) channel gating kinetics by the S3–S4 linker. *J. Gen. Physiol.* 115:193–208.

37. Mathur, R., J. Zheng, Y. Yan, and F. J. Sigworth. 1997. Role of the S3–S4 linker in *Shaker* potassium channel activation. *J. Gen. Physiol.* 109:191–199.

38. Sorensen, J. B., A. Cha, R. Latorre, E. Rosenman, and F. Bezanilla. 2000. Deletion of the S3–S4 linker in the *Shaker* potassium channel reveals two quenching groups near the outside of S4. *J. Gen. Physiol.* 115:209–222.

39. Kikuchi, K., T. Nagatomo, H. Abe, K. Kawakami, H. J. Duff, et al. 2005. Blockade of HERG cardiac K^+ current by antifungal drug miconazole. *Br. J. Pharmacol.* 144:840–848.

40. Alexandrou, A. J., R. S. Duncan, A. Sullivan, J. C. Hancox, D. J. Leishman, et al. 2006. Mechanism of hERG K^+ channel blockade by the fluoroquinolone antibiotic moxifloxacin. *Br. J. Pharmacol.* 147:905–916.

41. Milnes, J. T., O. Crociani, A. Arcangeli, J. C. Hancox, and H. J. Witchel. 2003. Blockade of HERG potassium currents by fluvoxamine: incomplete attenuation by S6 mutations at F656 or Y652. *Br. J. Pharmacol.* 139:887–898.

42. Duncan, R. S., M. J. McPate, J. M. Ridley, Z. Gao, A. F. James, et al. 2007. Inhibition of the HERG potassium channel by the tricyclic antidepressant doxepin. *Biochem. Pharmacol.* 74:425–437.